



Green Synthesis of Gold Nanoparticles using *Pimenta dioica* Leaves Aqueous Extract and Their Application as Photocatalyst, Antioxidant, and Antibacterial Agents

Adewale Fadaka*, Olukemi Aluko, Saartjie Awawu, and Karim Theledi

Received : February 19, 2021

Revised : March 23, 2021

Accepted : April 15, 2021

Online : April 17, 2021

Abstract

Green synthesis of gold nanoparticles (AuNPs) is of particular interest due to their catalytic, antioxidant, and antibacterial properties. In this study, the aqueous extract of *Pimenta dioica* leaves was used to synthesize AuNPs and the effective parameters were investigated. The prepared AuNPs were characterized by various techniques including UV-Vis absorption spectroscopy, Fourier Transform Infrared (FTIR) spectroscopy, Transmission Electron Microscopy (TEM), and X-ray diffractometer (XRD). The reduction and stabilization effect of the plant extract to fabricate AuNPs were explained by FTIR analysis. TEM imaging confirmed the formation of spherical-shaped AuNPs. The catalytic activity of synthesized nanoparticles was evaluated in the degradation of a methylene blue dye in the presence of NaBH₄ as reducing agent and achieved after only two minutes. The AuNPs provided high antioxidant ability. In addition, the synthesized AuNPs showed a significant inhibitory effect against both gram-positive and gram-negative bacteria, where the zone of inhibition of 4 and 9 mm were obtained for synthesized AuNPs against *S. aureus* and *E. coli*, respectively.

Keywords: antibacterial, antioxidant, catalyst, gold nanoparticles, *Pimenta dioica*

1. INTRODUCTION

Researchers are interested in gold nanoparticles (AuNPs) because of their applications in optoelectronic [1], electrical [2], and magnetic devices [3], as well as catalysis [4]–[6], sensors [7]–[9], and drug delivery [10]. Form, size, crystallinity, and structure are all important factors in these applications. Gold nanostructures have been identified in a variety of shapes, including nanocubes [11], nanowires [12], nanoplates [13], nanospheres, nanorods [14], nanopores [15], nanobelts, and odd angled shapes [16]. Many groups of researchers have long been interested in one-dimensional (1D) metallic nanostructures. The researchers were drawn to AuNPs because of their unusual and tunable surface plasmon resonance. Because of their non-cytotoxicity and biocompatibility, AuNPs have become more

common in biomedical applications than other metallic nanostructures [17]. AuNPs are simple to make and have excellent chemical and thermal stability. Because of their unusual biocompatibility and well-defined surface chemistry, AuNPs have been used as detection methods in molecular imaging using fluorescence resonance energy transfer [18].

Due to its unique characteristics such as safety, environmental friendliness, and cost-effectiveness, green synthesis of AuNPs has gotten a lot of attention [19][20]. For the synthesis of AuNPs, various physical and chemical methods have already been used [21]–[23]. Most of the approaches require long experiment time, involve a multi-step synthesis procedure, and use the harmful organic and inorganic chemicals [22]. The existence of these toxic chemicals in trace amounts on the surfaces of fabricated AuNPs is a possibility, which would restrict their biomedical applications. As a result, a method to synthesize biocompatible AuNPs that is both environmentally friendly and free of toxic chemicals is needed. Plant-mediated green synthesis is an environmentally friendly method for producing monodisperse and chemically stable AuNPs of various sizes and shapes. Plant phytochemicals or biomolecules play a key role in the reduction of metal ions during this synthesis phase [24].

Copyright Holder:

© Fadaka, A., Aluko, O., Awawu, S., and Theledi, K. (2021)

First Publication Right:

Journal of Multidisciplinary Applied Natural Science

Publisher's Note:

Pandawa Institute stays neutral with regard to jurisdictional claims in published maps and institutional affiliations.

This Article is Licensed Under:



Pimenta dioica (L.), also known as allspice, belongs to the Myrtaceae family. *P. dioica* has anesthetic, antiseptic, antihelmintic, febrifuge, and antiseptic properties. *P. dioica* dried fruits are a valuable spice used all over the world. The therapeutic properties of *P. dioica* fragrance oils include antioxidant, antimicrobial, tonic, hypotensive, anti-inflammatory, and anthelmintic properties [25].

Pimenta dioica has been used in the preparation of silver nanoparticles in previous studies [26]. Carbohydrate, protein, steroid, alkaloid, flavonoids, phenol, and terpenoids were detected in the ethanolic extract; protein, phenol, and terpenoids were detected in the diethyl ether extract; and carbohydrate, alkaloid, flavonoids, steroids, saponins, tannin, and terpenoids were detected in the aqueous extract. By using a ferrous ion chelating assay, a nitric oxide radical scavenging assay, and a DPPH test, the antioxidant content of *P. dioica* leaf extract was determined. The occurrence of carboxylic acid, alkyl halides alkanes, and miscellaneous functional groups in *P. dioica* leaves have been reported by Murali et al. [27]. Kharey et al. [28] obtain green synthesized AuNPs using aqueous leaf extract of *P. dioica*. Using MTT (3-(4,5-dimethylthiazol-2-yl)-2,5-diphenyl tetrazolium bromide) assay, synthesized AuNPs safe for human cervical cancer (HeLa) and human embryonic kidney 293 (HEK 293) cell lines. Further, the synthesized AuNPs showed excellent photoacoustic signal responses (PASR) and found to be the most efficient photoacoustic signal generators.

As a result, the aim of this study was to synthesize AuNPs from *P. dioica* leaf aqueous extract without using any other chemicals. Several spectral and microscopic methods revealed the formation of NPs. The effectiveness of AuNPs in reducing the organic dye pollutant methylene blue (MB) was also investigated. At the same time, the antioxidant and antibacterial properties of the synthesized AuNPs were examined.

2. MATERIALS AND METHODS

2.1. Materials

Pimenta dioica leaves were freshly collected from Lapai, Nigeria. Gold (III) chloride tri-hydrate

($\text{HAuCl}_4 \cdot 3\text{H}_2\text{O}$), 2,2-diphenyl-1-picrylhydrazyl (DPPH), methylene blue dyes (MB) and sodium borohydride (NaBH_4) were obtained from Sigma-Aldrich. Deionized ultra-pure water was used for preparing all respective solutions.

2.2. Methods

2.2.1. Preparation of aqueous extract

Under strict sterile conditions, about 25 g of fresh *P. dioica* leaves were softened in a mortar and pestle and filtered through muslin cloth. In a clean and fresh glass bottle, the filtrate was collected. This filtrate will be kept cold for further examination. Around 5 g of leaves were crushed and mixed with 10 mL of deionized ultra-pure water before being ground. The extraction process took 3 h and was held overnight. The solution was filtered the next day, and the filtrate was processed for further analysis.

2.2.2. Biosynthesis of AuNPs by *P. dioica* leaves aqueous extract

The reduction of Au^{3+} to Au^0 , as described by Jayaseelan et al. [29], was used to produce AuNPs mediated by *P. dioica* extract. As much as 40 mL of *P. dioica* leaves aqueous extract was added to 60 mL of 1 mM aqueous $\text{HAuCl}_4 \cdot 3\text{H}_2\text{O}$ solution and the solution was placed in orbital shaker at room temperature, for reduction of Au^{3+} to Au^0 . The bio-reduction of the gold ions in the solution was monitored periodically by measuring the UV-Visible (UV-Vis) spectroscopy of the solutions. The reaction was rapid as the ruby red color appeared within 10 min and the reaction confirmed the formation of Au NPs and there was no color change

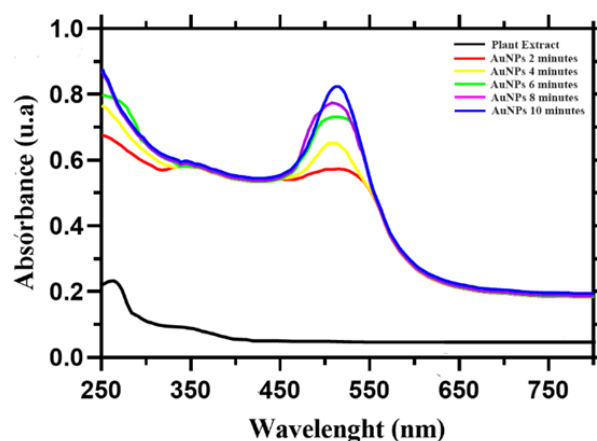


Figure 1. UV-Visible spectrum of synthesized AuNPs showed peak at 536 nm.

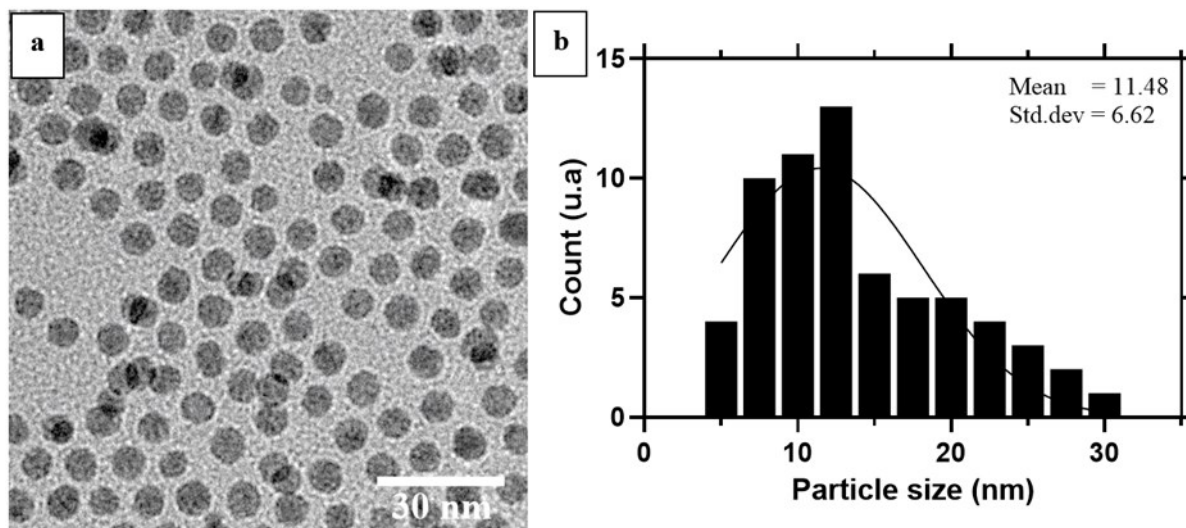


Figure 2. (a) TEM image and (b) particle size distribution of synthesized AuNPs.

further. The control leaves aqueous extract of *P. dioica* did not show any change in color. The optimum time required for the completion of reaction was 10 min. Different concentration of HAuCl₄ solution was used to get maximum AuNPs. The overall optimized reaction condition was observed in 1 mM HAuCl₄ solution and neutral pH. The AuNPs obtained from the solution were purified by repeated centrifugation at 2000 rpm for 10 min followed by dispersion of the pellet thrice in deionized ultra-pure water to remove the water-soluble biomolecules such as proteins and secondary metabolites. The water suspended AuNPs were frozen at 30 °C overnight and then kept under vacuum for 24 h to dry the AuNPs.

2.2.3. Characterization

The morphology of the synthesized AuNPs (including nanoscale, shape, and uniformity) was investigated by TEM microscope, (JEOL, model JEM-2010) with an accelerating voltage of 200 kV. The optical absorbance of the as-prepared NPs solutions was measured by UV-Vis spectrophotometer (Shimadzu UV-2450, one cm wide quartz cells). The structural information and types of functional groups from the extract that may be involved in the synthesis and stabilization of AuNPs were obtained by FTIR spectrophotometer (JASCO spectrometer) over the 4000 to 400 cm⁻¹ range. The particle size range of the nanoparticles were determined by using particle size analyzer (Malvern Zetasizer nanosizer).

2.2.4. The photocatalytic activity

The photocatalytic activity of AuNPs was assessed by investigating the reduction of MB dye via NaBH₄, whereas the biologically as-synthesized AuNPs were utilized as a catalyst at 25 °C under solar light. The procedure started by adding 2.5 mL of 0.08 mM MB dye solutions in a one cm path length quartz cuvette. Then, 0.5 mL of freshly prepared NaBH₄ (0.06 M) solution was added to the dye solution, followed by the addition of 0.5 mL of colloidal AuNPs. Afterward, the solution was subjected to solar light under gentle stirring. The dye's reduction reaction was monitored by recording changes in the MB absorption after one minute using the following Equation 1 [24]:

$$\text{degradation rate (\%)} = \frac{(C_0 - C)}{C_0} \times 100\% \quad (1)$$

While, C₀ = initial concentration of dye, C = the concentration of dye upon irradiation.

2.2.5. The Antioxidant efficiency

The free radical scavenging potential of the plant extract and prepared NPs were assessed using DPPH, according to Amrulloh et al. [30] method. Briefly, the synthesized AuNPs solution (different volume 10, 20, 30, 40, and 50 μL) was mixed with 1000 μL of DPPH (0.2 mM). A DPPH solution without NPs was also examined and utilized as a negative control. Additionally, the test was also made on two-fold-diluted solutions of each sample. After that, the DPPH solutions were blended for 20 min at ambient temperature in a dark condition. At

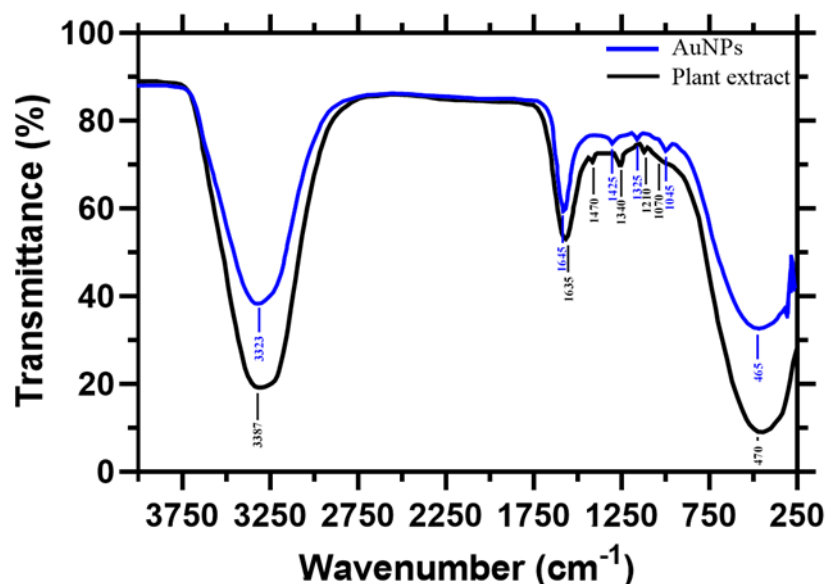


Figure 3. FTIR spectrum of synthesized AuNPs and *P. dioica* leaves aqueous extract.

the end of the incubation period, the radical concentration was determined by following the reduction in its absorbance percentage at a specific wavelength of 517 nm. The scavenging efficiency was expressed as the inhibition percent of DPPH radicals, and it was calculated according to the following Equation 2 [24]:

$$\% \text{ inhibition} = \frac{\text{control absorbance} - \text{sample absorbance}}{\text{control absorbance}} \times 100\% \quad (2)$$

2.2.6. The antibacterial assays

Antibacterial activity was analyzed with synthesized AuNPs by well diffusion method against clinically isolated Gram negative (*Escherichia coli*) and Gram positive (*Staphylococcus aureus*) microorganisms. The pathogenic cultures were bringing into broth culture for antibacterial assay. Approximately 7-mm diameter of well was made on Muller Hinton Agar plate with the help of gel puncture. The cultures were swabbed on test media with sterile cotton swab. Various volume (10, 20, 30, 40, and 50 μL) of synthesized AuNPs were inoculated to the well, and then the plates were incubated in incubator for 37 $^{\circ}\text{C}$ for 24 h, the zones of inhibition indicated the antibacterial activity was measured in mm.

3. RESULTS AND DISCUSSIONS

3.1. Spectral, morphological, and structural characterization

3.1.1. UV-Visible spectroscopy, TEM, and PSA

The green synthesis of AuNPs using environmental and nontoxic chemicals is the current approach. One of the most frequently used materials in green synthesis is the plant extract, which contains functional groups that can reduce Au^{3+} to Au^0 . The UV-Vis absorption spectra demonstrates a novel technique for the preparation of the Au NPs. The scale of wavelength was fixed between 250 and 800 nm, the surface plasmon resonance (SPR) of the AuNPs formed corresponded to 536 nm and there was an increase in intensity till 10 min as a function of time without any shift in the peak wavelength (Figure 1). It can be observed that the reduction of gold ions reaches saturation within 10 min of reaction, and after that, only slight variations can be noted in the intensity of SPR bands [24]. This result indicates that the reaction is completed in 10 min.

TEM images precisely reveal the morphological tuning with perpetual changes in synthesis conditions. Figure 2 shows TEM images of AuNPs. The particle size distributions of colloids AuNPs from PSA result are depicted in the histograms. The average particle size measured for AuNPs colloids is 11.48 nm.

3.1.2. FTIR spectroscopy and X-ray diffraction analysis

FTIR analysis was used to identify the possible bio-reducing biomolecules in the extract [31]. The

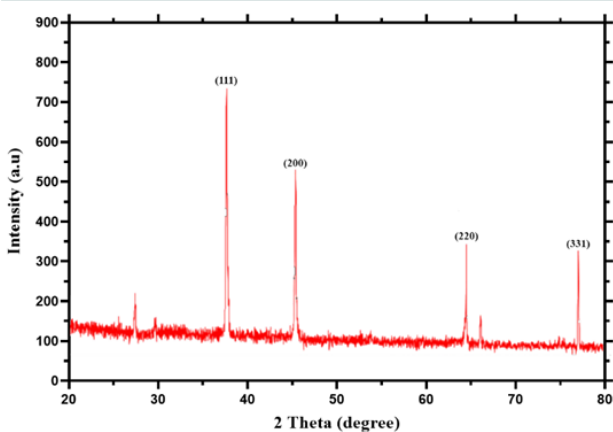


Figure 4. XRD pattern of synthesized AuNPs.

presence of functional groups on the surface of AuNPs was identified by the FTIR measurement of synthesized AuNPs. FTIR spectra of AuNPs and plant extract are displayed in Figure 3. The major peaks were found at 3387, 1635, 1470, 1340, 1210, and 1070 cm^{-1} respectively. The peak at 3387 cm^{-1} indicates the presence of OH (phenolic/aliphatic hydroxyl) group. The peak at 1635 cm^{-1} represents the -C=C stretching of the alkene bond in eugenol. The peak at 1470 cm^{-1} corresponds to -C-C bond of an aromatic ring. The peaks at 1340, 1210, and 1070 cm^{-1} correspond to the asymmetric and symmetric C-O-C stretching mode, respectively, which confirms the presence of the methoxy group on the benzene ring of eugenol [32]–[34]. These peaks are consistent with the FTIR peaks of functional groups of eugenol, present in the *P. dioica* plant [28].

The FTIR spectrum of AuNPs shows the peaks at 3323, 1645, 1425, 1325, and 1045 cm^{-1} respectively. A minor wavelength shift is observed in the peaks of the functional groups that were present in the extract before and after the nanoparticle formation. This peak shift could be attributed to the interaction of functional groups in *P. dioica* plant extract with the nanoparticles. The strong band at 3323 cm^{-1} is the characteristic band of phenolic compound while the weak band at 1645 cm^{-1} corresponds to the alkene group of eugenol constituent of plant extract [35]. Results suggested that eugenol not only helps in the reduction of gold ions but also stabilizes the AuNPs [36].

The structural phase of the AuNPs formed were studied through XRD analysis. Figure 4 shows the strong and narrow diffraction peaks indicated that the product has well crystalline. The XRD peaks at 38, 44, 64 and 77 ($^{\circ}$ 2theta) can be indexed to the (111), (200), (220) and (311) Bragg's reflections of sphere structure of metallic gold respectively (JCPDS no. 04-0784) [29]. The broadening of Bragg's peaks indicates the formation of AuNPs. Nearly monodispersed AuNPs with controllable size and uniform shape can be easily obtained in the simple aqueous reduction method.

3.2. The AuNPs Photocatalytic study for reduction of methylene blue

Contamination of water with organic dyes has become a formidable challenge in recent years.

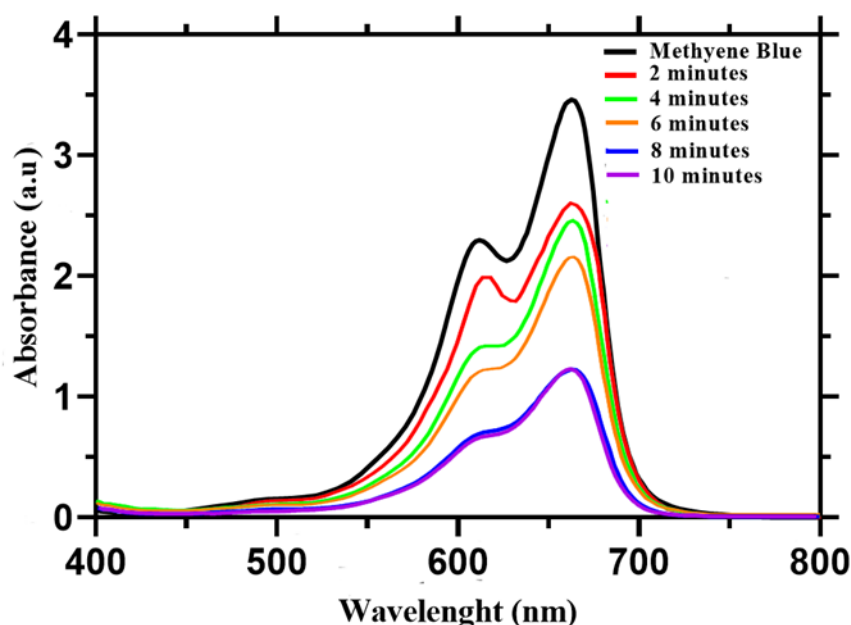


Figure 5. Absorbance spectra of photocatalytic degradation for MB dye in the presence of AuNPs.

Table 1. The DPPH scavenging activity of synthesized AuNPs.

Sample	Concentration ($\mu\text{g/mL}$)	DPPH scavenging activity (%)
<i>P. dioica</i> leave aqueous extract	50	68.87 ± 0.21
	100	72.37 ± 0.15
	150	78.15 ± 0.31
AuNPs	50	10.61 ± 0.10
	100	18.54 ± 0.24
	150	37.43 ± 0.42

Methylene blue (MB) was chosen as the subject of our study because it is one of the most widely used organic dyes in many industries, and its residue in wastewater is considered toxic contamination. The MB was widely used in industry as a redox indicator, and the traditional method for removing it from wastewater was to use a reducing agent like NaBH_4 , which produces hydrogen gas through a hydrolysis reaction in aqueous solution. The catalytic activity of AuNPs in the presence of NaBH_4 is investigated in this study. The absorption spectrum of MB is well known for having a peak at 664 nm attributed to the $n-\pi^*$ transition and another shoulder peak at 614 nm [29]. In the presence of NaBH_4 , this peak gradually decreases due to the formation of the reduced form known as leuco methylene blue (LMB) [37]. Nonetheless, it was discovered that the rate of reduction by NaBH_4 was slow and prolonged. AuNPs have been used as a catalytic material. The resulting absorption spectra is plotted in Figure 5. The blue color of the MB and NaBH_4 solution was observed to vanish when sample from prepared AuNPs was added to the solution. After two minutes, the intensity of the peak at 664 nm reduced, indicating that the AuNPs were an active catalyst for MB reduction. Following the control sample (NaBH_4 solution without any AuNPs), a 73% reduction was obtained after 8 min and it remained unchanged for 10 min. Accordingly, a clear improvement and enhancement were obtained due to the addition of the AuNPs.

3.3. Antioxidant activity

It has been documented that a reactive oxygen species and other free radicals may be formed and released during a variety of biological processes, resulting in pathogenicity [36][37]. Antioxidant

behavior refers to the formation of non-reactive and stable radicals as a result of the inhibition of any molecule's oxidation mechanism. This is accomplished by preventing the oxidative chain reaction's initiation step. As a result, considerable effort was expended in the quest for an antioxidant agent capable of obstructing or preventing oxidative harm [40]. It was recently discovered that AuNPs, especially those prepared in a green route, have significant antioxidant potential, which is dependent on the properties of various phytochemicals encrusted on the surface of the AuNPs [24][39][40]. The DPPH assay is a quick and easy way to figure out the preliminary results. The synthesized AuNPs in this study have a higher propensity for scavenging DPPH (Table 1). The colloids scavenging action increases as the concentration of the synthesized gold colloid rises. Tannins and polyphenols are abundantly found in the aqueous extract of *P. dioica* leaves [27]. These bioactive compounds synergic activity as a reducing and stabilizing agent has been predicted.

3.4. Antibacterial activity

Noble metals and their compounds exhibit antimicrobial properties, allowing them to be used to treat burns and chronic wounds. Metal nanoparticles' superior biological performance is reported due to their high surface area to volume ratio as compared to their bulkier counterparts [43]–[45]. The antibacterial activity of synthesized AuNPs was tested on a variety of bacteria in this study under agar well diffusion method. Table 2 shows antibacterial effect of bioinspired AuNPs on different human pathogens *S. aureus* and *E. coli*. For an addition of 30 $\mu\text{g/mL}$ of the gold colloid, an inhibition zone of 4 mm *S. aureus* and 9 mm for

Table 2. Antibacterial activity of AuNPs.

Bacteria	Zone of Inhibition (mm)				
	Distilled water	Amphotericin B (20 µg/ml)	AuNPs (10 µg/ml)	AuNPs (20 µg/ml)	AuNPs (30 µg/ml)
<i>Staphylococcus aureus</i>	-	12 ± 1.0	-	2 ± 1.0	4 ± 0.5
<i>Escherichia coli</i>	-	14 ± 1.0	2 ± 0.5	6 ± 1.0	9 ± 1.0

E.coli was observed. The mechanism behind AuNPs' bactericidal effect has yet to be fully investigated. However, earlier studies cite many reasons for the impact in a hazy depiction of the process. AuNPs have been documented to bind to the cell membrane's surface and disrupt key functions such as permeability and respiration, resulting in antioxidant depletion and the development of reactive oxygen species (ROS) [46]. Metal nanoparticles can also release metal ions, which can penetrate the cell wall and cause DNA damage and protein malfunction. The surface area available for touch determines how well the particles stick to the bacteria. As a result, smaller AuNPs with a higher surface area will have a stronger bactericidal impact than larger AuNPs [47]. The present study clearly indicates that the synthesized AuNPs show good activity against both gram-positive and gram-negative bacteria.

4. CONCLUSIONS

In summary, AuNPs were successfully biosynthesized by an inexpensive, fast, and safe approach, using *Pimenta dioica* leaves aqueous extract, without the use of any toxic chemicals. TEM imaging revealed that these AuNPs have spherical structure. Moreover, FTIR analysis suggested that the surface of AuNPs is covered by biomolecules found in the plant extract such as phenolics and eugenols. These AuNPs have demonstrated an excellent catalytic activity for the degradation of MB. Additionally, AuNPs displayed the most potent antioxidant potential. Also, an antibacterial inhibition was evident against gram-positive and gram-negative pathogenic.

AUTHOR INFORMATION

Corresponding Author

Adewale Fadaka — Department of Chemistry, Ibrahim Badamasi Babangida University Lapai, Lapai – 911101 (Nigeria);
Email: adewalefad@ibbu.edu.ng

Authors

Olukemi Aluko — Department of Chemistry, Ibrahim Badamasi Babangida University Lapai, Lapai – 911101 (Nigeria);

Saartjie Awawu — Department of Chemistry, Ibrahim Badamasi Babangida University Lapai, Lapai – 911101 (Nigeria);

Karim Theledi — Department of Biotechnology, University of the Western Cape, Bellville – 7530 (South Africa);

REFERENCES

- [1] R. C. Sanfelice, L. A. Mercante, A. Pavinatto, N. B. Tomazio, C. R. Mendonça, S. J. L. Ribeiro, L. H. C. Mattoso, and D. S. Correa. (2017). "Hybrid composite material based on polythiophene derivative nanofibers modified with gold nanoparticles for optoelectronics applications". *Journal of Materials Science*. **52** (4): 1919–1929. [10.1007/s10853-016-0481-8](https://doi.org/10.1007/s10853-016-0481-8).
- [2] C. C. D. Wang, W. C. H. Choy, C. Duan, D. D. S. Fung, W. E. I. Sha, F. X. Xie, F. Huang, and Y. Cao. (2012). "Optical and electrical effects of gold nanoparticles in the active layer of polymer solar cells". *Journal of Materials Chemistry*. **22** (3): 1206–1211. [10.1039/C1JM14150C](https://doi.org/10.1039/C1JM14150C).
- [3] K. Pungjunun, S. Chaiyo, I. Jantrahong, S. Nantaphol, W. Siangproh, and O. Chailapakul. (2018). "Anodic stripping

- voltammetric determination of total arsenic using a gold nanoparticle-modified boron-doped diamond electrode on a paper-based device". *Microchimica Acta*. **185** (7): 324. [10.1007/s00604-018-2821-7](https://doi.org/10.1007/s00604-018-2821-7).
- [4] H. R. M. Jhong, C. E. Tornow, C. Kim, S. Verma, J. L. Oberst, P. S. Anderson, A. A. Gewirth, T. Fujigaya, N. Nakashima, and P. J. A. Kenis. (2017). "Gold Nanoparticles on Polymer-Wrapped Carbon Nanotubes: An Efficient and Selective Catalyst for the Electroreduction of CO₂". *ChemPhysChem*. **18** (22): 3274–3279. [10.1002/cphc.201700815](https://doi.org/10.1002/cphc.201700815).
- [5] T. D. Tran, M. T. T. Nguyen, H. V. Le, D. N. Nguyen, Q. D. Truong, and P. D. Tran. (2018). "Gold nanoparticles as an outstanding catalyst for the hydrogen evolution reaction". *Chemical Communications*. **54** (27): 3363–3366. [10.1039/c8cc00038g](https://doi.org/10.1039/c8cc00038g).
- [6] M. Gholinejad, N. Dasvarz, M. Shojafar, and J. M. Sansano. (2019). "Starch functionalized creatine for stabilization of gold nanoparticles: Efficient heterogeneous catalyst for the reduction of nitroarenes". *Inorganica Chimica Acta*. **495**. [10.1016/j.ica.2019.118965](https://doi.org/10.1016/j.ica.2019.118965).
- [7] B. Li, X. Li, Y. Dong, B. Wang, D. Li, Y. Shi, and Y. Wu. (2017). "Colorimetric Sensor Array Based on Gold Nanoparticles with Diverse Surface Charges for Microorganisms Identification". *Analytical Chemistry*. **89** (20): 10639–10643. [10.1021/acs.analchem.7b02594](https://doi.org/10.1021/acs.analchem.7b02594).
- [8] X. Niu, Y. Zhong, R. Chen, F. Wang, Y. Liu, and D. Luo. (2018). "A 'turn-on' fluorescence sensor for Pb²⁺ detection based on graphene quantum dots and gold nanoparticles". *Sensors Actuators B Chemical*. **255** : 1577–1581. [10.1016/j.snb.2017.08.167](https://doi.org/10.1016/j.snb.2017.08.167).
- [9] Y. Xu, F. Y. H. Kutsanedzie, M. Hassan, J. Zhu, W. Ahmad, H. Li, and Q. Chen. (2020). "Mesoporous silica supported orderly-spaced gold nanoparticles SERS-based sensor for pesticides detection in food". *Food Chemistry*. **315** : 126300. [10.1016/j.foodchem.2020.126300](https://doi.org/10.1016/j.foodchem.2020.126300).
- [10] M. Sharifi, F. Attar, A. A. Saboury, K. Akhtari, N. Hooshman, A. Hasan, M. A. El-Sayed, and M. Falahati. (2019). "Plasmonic gold nanoparticles: Optical manipulation, imaging, drug delivery and therapy". *Journal of Controlled Release*. **311–312** : 170–189. [10.1016/j.jconrel.2019.08.032](https://doi.org/10.1016/j.jconrel.2019.08.032).
- [11] H. Bin Jeon, P. V. Tsalu, and J. W. Ha. (2019). "Shape Effect on the Refractive Index Sensitivity at Localized Surface Plasmon Resonance Inflection Points of Single Gold Nanocubes with Vertices". *Scientific Reports*. **9** (1): 13635. [10.1038/s41598-019-50032-3](https://doi.org/10.1038/s41598-019-50032-3).
- [12] M. D. Ho, Y. Ling, L. W. Yap, Y. Wang, D. Dong, Y. Zhao, and W. Cheng. (2017). "Percolating Network of Ultrathin Gold Nanowires and Silver Nanowires toward 'Invisible' Wearable Sensors for Detecting Emotional Expression and Apexcardiogram". *Advanced Functional Materials*. **27** (25): 1700845. [10.1002/adfm.201700845](https://doi.org/10.1002/adfm.201700845).
- [13] M. M. Chen, W. Zhao, M. J. Zhu, X. L. Li, C. H. Xu, H. Y. Chena, and J. J. Xu. (2019). "Spatiotemporal imaging of electrocatalytic activity on single 2D gold nanoplates via electrogenerated chemiluminescence microscopy". *Chemical Science*. **10** (15): 4141–4147. [10.1039/C9SC00889F](https://doi.org/10.1039/C9SC00889F).
- [14] A. P. Sangnier, A. V. Walle, R. Aufaure, M. Fradet, L. Motte, E. Guénin, Y. Lalatonne, and C. Wilhelm. (2020). "Photothermal Therapy: Endosomal Confinement of Gold Nanospheres, Nanorods, and Nanoraspberries Governs Their Photothermal Identity and Is Beneficial for Cancer Cell Therapy". *Advanced Biosystems*. **4** (4): 2070042. [10.1002/adbi.202070042](https://doi.org/10.1002/adbi.202070042).
- [15] H. L. Liu, J. Cao, S. Hanif, C. Yuan, J. Pang, R. Levicky, X. H. Xia, and K. Wang. (2018). "Size-Controllable Gold Nanopores with High SERS Activity". *Analytical Chemistry*. **89** (19): 10407–10413. [10.1021/acs.analchem.7b02410](https://doi.org/10.1021/acs.analchem.7b02410).
- [16] W. Xin, I. M. De Rosa, P. Ye, J. Severino, C. Li, X. Yin, M. S. Goorsky, L. Carlson, and J. M. Yang. (2018). "Graphene

- template-induced growth of single-crystalline gold nanobelts with high structural tunability”. *Nanoscale*. **10** (6): 2764–2773. [10.1039/C7NR07514F](https://doi.org/10.1039/C7NR07514F).
- [17] N. Elahi, M. Kamali, and M. H. Baghersad. (2018). “Recent biomedical applications of gold nanoparticles: A review”. *Talanta*. **184** : 537–556. [10.1016/j.talanta.2018.02.088](https://doi.org/10.1016/j.talanta.2018.02.088).
- [18] Q. Zhang, Y. Gong, X. Guo, P. Zhang, and C. Ding. (2018). “Multifunctional Gold Nanoparticle-Based Fluorescence Resonance Energy-Transfer Probe for Target Drug Delivery and Cell Fluorescence Imaging”. *ACS Applied Materials & Interfaces*. **10** (41): 34840–34848. [10.1021/acscami.8b12897](https://doi.org/10.1021/acscami.8b12897).
- [19] Z. Molnár, V. Bódai, G. Szakacs, B. Erdélyi, Z. Fogarassy, G. Sáfrán, T. Varga, Z. Kónya, E. T. Szeles, R. Szűcs, and I. Lagzi. (2018). “Green synthesis of gold nanoparticles by thermophilic filamentous fungi”. *Scientific Reports*. **8** (1): 3943. [10.1038/s41598-018-22112-3](https://doi.org/10.1038/s41598-018-22112-3).
- [20] J. Santhoshkumar, S. Rajeshkumar, and S. Venkat Kumar. (2017). “Phyto-assisted synthesis, characterization and applications of gold nanoparticles – A review”. *Biochemistry and Biophysics Reports*. **11** : 46–57. [10.1016/j.bbrep.2017.06.004](https://doi.org/10.1016/j.bbrep.2017.06.004).
- [21] L. Freitas de Freitas, G. Varca, J. dos Santos Batista, and A. Benévolo Lugão. (2018). “An Overview of the Synthesis of Gold Nanoparticles Using Radiation Technologies”. *Nanomaterials*. **8** (11): 939. [10.3390/nano8110939](https://doi.org/10.3390/nano8110939).
- [22] C. Daruich De Souza, B. Ribeiro Nogueira, and M. E. C. M. Rostelato. “Review of the methodologies used in the synthesis gold nanoparticles by chemical reduction”. *Journal of Alloys and Compounds*. **798** : 714–740. [10.1016/j.jallcom.2019.05.153](https://doi.org/10.1016/j.jallcom.2019.05.153).
- [23] M. Ali Dheyab, A. Abdul Aziz, P. Moradi Khaniabadi, M. S. Jameel, N. M. Ahmed, and A. Taha Ali. (2021). “Distinct advantages of using sonochemical over laser ablation methods for a rapid-high quality gold nanoparticles production”. *Materials Research Express*. **8** (1): 015009. [10.1088/2053-1591/abd5a4](https://doi.org/10.1088/2053-1591/abd5a4).
- [24] O. M. El-Borady, M. S. Ayat, M. A. Shabrawy, and P. Millet. (2020). “Green synthesis of gold nanoparticles using Parsley leaves extract and their applications as an alternative catalytic, antioxidant, anticancer, and antibacterial agents”. *Advanced Powder Technology*. **31** (10): 4390–4400. [10.1016/j.apt.2020.09.017](https://doi.org/10.1016/j.apt.2020.09.017).
- [25] C. Dima, M. Cotârlet, P. Alexe, and S. Dima. (2014). “Microencapsulation of essential oil of pimento [*Pimenta dioica* (L) Merr.] by chitosan/k-carrageenan complex coacervation method”. *Innovative Food Science & Emerging Technologies*. **22** : 203–211. [10.1016/j.ifset.2013.12.020](https://doi.org/10.1016/j.ifset.2013.12.020).
- [26] R. Li, Y. Pan, N. Li, Q. Wang, Y. Chen, M. Phisalaphong, and H. Chen. (2020). “Antibacterial and cytotoxic activities of a green synthesized silver nanoparticles using corn silk aqueous extract,” *Colloids and Surfaces A: Physicochemical and Engineering Aspects*. **598** : 124827. [10.1016/j.colsurfa.2020.124827](https://doi.org/10.1016/j.colsurfa.2020.124827).
- [27] V. S. Murali, V. N. Meena Devi, P. Parvathy, and M. Murugan. (2020). “Phytochemical screening, FTIR spectral analysis, antioxidant and antibacterial activity of leaf extract of *Pimenta dioica* Linn”. *Materials Today: Proceedings*. [10.1016/j.matpr.2020.10.038](https://doi.org/10.1016/j.matpr.2020.10.038).
- [28] P. Kharey, S. B. Dutta, A. Gorey, M. Manikandan, A. Kumari, S. Vasudevan, I. A. Palani, S. K. Majumder, and S. Gupta. (2020). “*Pimenta dioica* Mediated Biosynthesis of Gold Nanoparticles and Evaluation of Its Potential for Theranostic Applications”. *ChemistrySelect*. **5** (26): 7901–7908. [10.1002/slct.202001230](https://doi.org/10.1002/slct.202001230).
- [29] C. Jayaseelan, R. Ramkumar, A. A. Rahuman, and P. Perumal. (2013). “Green synthesis of gold nanoparticles using seed aqueous extract of *Abelmoschus esculentus* and its antifungal activity”. *Industrial Crops and Products*. **45** : 423–429. [10.1016/j.indcrop.2012.12.019](https://doi.org/10.1016/j.indcrop.2012.12.019).
- [30] H. Amrulloh, A. Fatiqin, W. Simanjuntak, H. Afriyani, and A. Annissa. (2021). “Bioactivities of nano-scale magnesium

- oxide prepared using aqueous extract of *Moringa Oleifera* leaves as green agent”. *Advances in Natural Sciences: Nanoscience and Nanotechnology*. **12** (1): 015006. [10.1088/2043-6254/abde39](https://doi.org/10.1088/2043-6254/abde39).
- [31] V. Thi Lan Huong and N. T. Nguyen. (2020). “Green synthesis, characterization and antibacterial activity of silver nanoparticles using *Sapindus mukorossi* fruit pericarp extract”. *Materials Today: Proceedings*. [10.1016/j.matpr.2020.10.015](https://doi.org/10.1016/j.matpr.2020.10.015).
- [32] S. U. Ganaie, T. Abbasi, and S. A. Abbasi. (2015). “Green Synthesis of Silver Nanoparticles Using an Otherwise Worthless Weed *Mimosa pudica*): Feasibility and Process Development Toward Shape/Size Control”. *Particulate Science and Technology*. **33** (6): 638–644. [10.1080/02726351.2015.1016644](https://doi.org/10.1080/02726351.2015.1016644).
- [33] K. O. Shittu, M. T. Bankole, A. S. Abdulkareem, O. K. Abubakre, and A. U. Ubaka. (2017). “Application of gold nanoparticles for improved drug efficiency”. *Advances in Natural Sciences: Nanoscience and Nanotechnology*. **8** (3): 035014. [10.1088/2043-6254/aa7716](https://doi.org/10.1088/2043-6254/aa7716).
- [34] B. Sundararajan and B. D. Ranjitha Kumari. (2017). “Novel synthesis of gold nanoparticles using *Artemisia vulgaris* L. leaf extract and their efficacy of larvicidal activity against dengue fever vector *Aedes aegypti* L.”. *Journal of Trace Elements in Medicine and Biology*. **43** : 187–196. [10.1016/j.jtemb.2017.03.008](https://doi.org/10.1016/j.jtemb.2017.03.008).
- [35] A. Marchese, R. Barbieri, E. Coppo, I. E. Orhan, M. Daglia, S. F. Nabavi, M. Izadi, M. Abdollahi, S. M. Nabavi, and M. Ajami. (2017). “Antimicrobial activity of eugenol and essential oils containing eugenol: A mechanistic viewpoint,” *Critical Reviews in Microbiology*. **43** (6): 668–689. [10.1080/1040841X.2017.1295225](https://doi.org/10.1080/1040841X.2017.1295225).
- [36] M. Parlinska-Wojtan, J. Depciuch, B. Fryc, and M. Kus-Liskiewicz. (2018). “Green synthesis and antibacterial effects of aqueous colloidal solutions of silver nanoparticles using clove eugenol”. *Applied Organometallic Chemistry*. **32** (4): e4276. [10.1002/aoc.4276](https://doi.org/10.1002/aoc.4276).
- [37] Y. Galagan and W.-F. Su. “Reversible photoreduction of methylene blue in acrylate media containing benzyl dimethyl ketal”. *Journal of Photochemistry and Photobiology A: Chemistry*. **195** (2–3): 378–383. [10.1016/j.jphotochem.2007.11.005](https://doi.org/10.1016/j.jphotochem.2007.11.005).
- [38] G. M. Sulaiman, W. H. Mohammed, T. R. Marzoog, A. A. A. Al-Amiery, A. A. H. Kadhum, and A. B. Mohamad. (2013). “Green synthesis, antimicrobial and cytotoxic effects of silver nanoparticles using *Eucalyptus chapmaniana* leaves extract”. *Asian Pacific Journal of Tropical Biomedicine*. **3** (1): 58–63. [10.1016/S2221-1691\(13\)60024-6](https://doi.org/10.1016/S2221-1691(13)60024-6).
- [39] P. Velmurugan, M. Iydroose, S. M. Lee, M. Cho, J. H. Park, V. Balachandar, and B.T. Oh. (2014). “Synthesis of Silver and Gold Nanoparticles Using Cashew Nut Shell Liquid and Its Antibacterial Activity Against Fish Pathogens,” *Indian Journal of Microbiology*. **54** (2): 196–202. [10.1007/s12088-013-0437-5](https://doi.org/10.1007/s12088-013-0437-5).
- [40] S. I. Yamagishi and T. Matsui. (2011). “Nitric oxide, a janus-faced therapeutic target for diabetic microangiopathy - Friend or foe?”. *Pharmacological Research*. **64** (3): 187–194. [10.1016/j.phrs.2011.05.009](https://doi.org/10.1016/j.phrs.2011.05.009).
- [41] K. Baek and J. K. Patra. (2015). “Novel green synthesis of gold nanoparticles using *Citrullus lanatus* rind and investigation of proteasome inhibitory activity, antibacterial, and antioxidant potential”. *International Journal of Nanomedicine*. **10** (1). 7253–7264. [10.2147/IJN.S95483](https://doi.org/10.2147/IJN.S95483).
- [42] G. Sathishkumar, K. J. Pradeep, V. Vignesh, C. Rajkuberan, M. Jeyaraj, M. Selvakumar, J. Rakhi, and S. Sivaramakrishnan. (2016). “Cannonball fruit (*Couroupita guianensis*, Aubl.) extract mediated synthesis of gold nanoparticles and evaluation of its antioxidant activity”. *Journal of Molecular Liquids*. **215** : 229–236. [10.1016/j.molliq.2015.12.043](https://doi.org/10.1016/j.molliq.2015.12.043).
- [43] X. Li, G. Gao, C. Sun, Y. Zhu, L. Qu, F. Jiang, and H. Ding. (2015). “Preparation and antibacterial performance testing of Ag nanoparticles embedded biological materials”. *Applied Surface Science*. **330** :

- 237–244. [10.1016/j.apsusc.2015.01.004](https://doi.org/10.1016/j.apsusc.2015.01.004).
- [44] N. Rahbar, L. Nazernezhad, M. Asadinezhad, Z. Ramezani, and M. Kouchak. (2018). “A novel micro-extraction strategy for extraction of bisphosphonates from biological fluids using zirconia nanoparticles coupled with spectrofluorimetry and high performance liquid chromatography”. *Journal of Food and Drug Analysis*. **26** (4): 1303–1311. [10.1016/j.jfda.2018.03.005](https://doi.org/10.1016/j.jfda.2018.03.005).
- [45] E. Inclan and M. Yoon. (2019). “Performance of biologically inspired algorithms tuned on TiO₂ nanoparticle benchmark system”. *Computational Materials Science*. **165** : 63–73. [10.1016/j.commatsci.2019.03.017](https://doi.org/10.1016/j.commatsci.2019.03.017).
- [46] M. Misawa and J. Takahashi. (2011). “Generation of reactive oxygen species induced by gold nanoparticles under x-ray and UV Irradiations”. *Nanomedicine: Nanotechnology, Biology and Medicine*. **7** (5): 604–614. [10.1016/j.nano.2011.01.014](https://doi.org/10.1016/j.nano.2011.01.014).
- [47] H. F. M. Xavier, V. M. Nadar, P. Patel, D. Umapathy, A. V. Joseph, S. Manivannan, P. Santhiyagu, B. Pandi, G. Muthusamy, Y. Rathinam, and K. Ponnuchamy. (2020). “Selective antibacterial and apoptosis-inducing effects of hybrid gold nanoparticles – A green approach”. *Journal of Drug Delivery Science and Technology*. **59** : 101890. [10.1016/j.jddst.2020.101890](https://doi.org/10.1016/j.jddst.2020.101890).